HHS Public Access

Author manuscript

Kidney Int. Author manuscript; available in PMC 2019 June 01.

Published in final edited form as:

Kidney Int. 2018 June ; 93(6): 1367–1383. doi:10.1016/j.kint.2017.12.017.

Activated renal tubular Wnt/β-catenin signaling triggers renal inflammation during overload proteinuria

Dickson W. L. Wong[1,2], **Wai Han Yiu**[1,2], **Kam Wa Chan**[1,2], **Ye Li**[1], **Bin Li**[1], **Sarah W.Y. Lok**[1], **Makoto M. Taketo**[3], **Peter Igarashi**[4], **Loretta Y. Y. Chan**[1], **Joseph C. K. Leung**[1], **Kar Neng Lai**[1], and **Sydney C. W. Tang**[1,2,*]

[1]Department of Medicine, The University of Hong Kong, Queen Mary Hospital, Hong Kong

[2]The University of Hong Kong Shenzhen Institute of Research and Innovation, China

[3]Division of Experimental Therapeutics, Graduate School of Medicine, Kyoto University, Yoshida-Konoé-cho, Sakyo, Kyoto 606-8501, Japan

[4]Department of Medicine, University of Minnesota Medical School, Minneapolis, Minnesota 55416, USA

Abstract

Imbalance of Wnt/β-catenin signaling in renal cells is associated with renal dysfunction, yet the precise mechanism is poorly understood. Previously we observed activated Wnt/β-catenin signaling in renal tubules during proteinuric nephropathy with an unknown net effect (rescue *vs.* damage?). To identify the definitive role of tubular Wnt/β-catenin, we generated a novel transgenic "Tubcat" mouse, which conditionally expresses stabilized β-catenin specifically in renal tubules after tamoxifen administration. Four weeks after tamoxifen injection, uninephrectomized Tubcat mice displayed proteinuria and elevated BUN levels comparing to non-transgenic mice, implying a detrimental effect of the activated signaling. This was associated with tubulointerstitial infiltration predominantly by M1 macrophages and overexpression of the inflammatory chemocytokines CCL-2 and RANTES. Induction of overload proteinuria by low-endotoxin BSA injection, after uninephrectomy, for 4 weeks aggravated proteinuria and increased BUN levels to a significantly greater extent in Tubcat mice. Renal dysfunction correlated with the degree of M1 macrophage infiltration in the tubulointerstitium and renal cortical up-regulation of CCL-2, IL-17A, IL-1β, CXCL1 and ICAM-1. There was overexpression of cortical TLR-4 and NLRP-3 in Tubcat mice, independent of BSA injection. Finally, there is no fibrosis formation or activation of epithelial-mesenchymal-transition or non-canonical Wnt pathways being observed in the Tubcat kidney. In conclusion, conditional activation of renal tubular Wnt/β-catenin signaling in a novel transgenic mouse model demonstrates that this pathway enhances intrarenal inflammation via the TLR-4/NLRP-3 inflammasome axis in overload proteinuria.

*Corresponding author: Sydney C.W. Tang, Division of Nephrology, Department of Medicine, The University of Hong Kong, Queen Mary Hospital, 102 Pokfulam Road, Hong Kong., Phone: +852-22553879; Fax: +852-28162863; scwtang@hku.hk.

DISCLOSURE: None.

Keywords

Wnt/β-catenin; renal inflammation; proteinuric nephropathy

INTRODUCTION

Persistent albuminuria is a surrogate marker of progressive chronic kidney disease (CKD) and its amelioration has been consistently associated with improved renal outcomes in both diabetic and non-diabetic CKD.[1] Excessive protein trafficking across the glomerular filtration barrier causes tubulotoxicity and drives progressive nephropathy[2] by triggering renal inflammation and subsequent fibrosis leading to eventual organ failure.[3]

In health, albumin is reabsorbed via receptor-mediated endocytosis by the proximal tubule followed by lysosomal degradation.[4, 5] In CKD patients, excessive albumin trafficking overwhelms the albumin handling capacity of renal tubules and mandates an array of detrimental intracellular signaling cascades in tubular cells,[6–9] including the hyperproduction of numerous chemocytokines that confer a pro-inflammatory microenvironment to enhance the transmigration of immune cells.[10] In particular, the macrophage was postulated to be the origin of myofibroblast accumulation that perpetuates excessive extracellular matrix protein deposition in the renal tubulointerstitium.[11]

Wnt/β-catenin signaling is highly conserved during embryonic development[12] and regulates different organogenesis.[13] There are several non-canonical Wnt pathways[14] which may cross talk with the Wnt/β-catenin signaling but the mechanisms are still rudimentary. Reports on the role of aberrant canonical Wnt/β-catenin signaling in different nephropathies have yielded contradicting results,[15–18] such that a consensus has not been reached.[19] Both podocyte-specific β-catenin overexpression or knock-out[15] and tubule-specific β-catenin knock-out mice[20] developed more severe renal dysfunction. Therefore, it has been postulated that an imbalance of Wnt/β-catenin signaling gives rise to nephropathy.[21]

Activated Wnt/β-catenin signaling is defined by stabilization and nuclear translocation of β-catenin followed by transcription of Wnt target genes. To avoid excessive accumulation of β-catenin in the cell, the serine/threonine sites on β-catenin, encoded by exon 3 within the *Catnb* allele,[22] are phosphorylated which will trigger ubiquitination and proteasomal degradation.[23]

Recent data support a reciprocal link between renal fibrosis and activated canonical Wnt/β-catenin signaling pathway in renal tubular cells.[24, 25] In this regard, we previously reported dynamic renal tubular Wnt/β-catenin signaling in proteinuric nephropathy.[26] Activated signaling occurred during the early onset of disease but regressed during the later phase. This signified that suppressed Wnt/β-catenin activity is associated with heightened tubular cell death and exacerbates proteinuria. Regardless of the fibrogenesis, activated Wnt/β-catenin signaling participates in a range of inflammatory diseases.[27–29] In addition, renal inflammation was observed in the early phase of proteinuric nephropathy in mice[30] and rats.[9, 31]

To provide a definitive role of Wnt/β-catenin signaling in kidney inflammation associated with heavy proteinuria, we generated a transgenic mouse strain which could be induced with tamoxifen to overexpress β-catenin exclusively in renal tubules, namely the Tubcat mouse. Tubcat mice were subjected to protein overload which recapitulates many features of CKD. We demonstrated that over-activated Wnt/β-catenin signaling in renal tubules exacerbates renal dysfunction. Importantly, the activated signaling *per se* is sufficient to propagate macrophage infiltration and increase chemocytokine levels in the kidney. In the protein overload model, Tubcat mice demonstrated further renal dysfunctions with more intense renal inflammation.

RESULTS

Generation and characterization of a conditional Tubcat mouse (Ksp-CreER^{T2}-Catnb$^{lox(ex3)/wt}$)

We successfully generated the first mouse strain that conditionally overexpresses β-catenin in renal tubules upon tamoxifen administration. As shown in Supplementary Figure 1A, mice carrying *loxP* sites flanking the exon 3 sequence of *Catnb* with (Tubcat) or without the *Ksp-Cre* allele (Cre$^{-/-}$; non-transgenic) were genotyped. Four weeks after tamoxifen administration, genomic DNA was extracted from the kidney, heart, spleen and liver. An additional PCR product corresponding to the recombined *Catnb* allele (~500bp) was evident in the genomic DNA of Tubcat mice from the kidney (Supplementary Figure 1B), but not in the tissue of heart, spleen and liver. This smaller size of the PCR product indicated the absence of exon 3 in the *Catnb* allele (*Catnb*$^{\Delta exon3}$) only in the kidney of Tubcat mice. Real-time PCR also showed that the expression of *Catnb exon 3* mRNA was significantly less in the kidney cortex of Tubcat mice versus Cre$^{-/-}$ mice (Figure 1A). Using immunoblotting assay, we detected the mutant form of β-catenin in the renal cortex of Tubcat mice (Figure 1B). Notably, colocalization by immunohistochemistry (IHC) staining of β-catenin and sodium chloride cotransporter (NCC) on the kidney sections (Figure 1C) revealed that up-regulated β-catenin expression was observed in renal tubules (both proximal and distal) of Tubcat mice. These results confirmed the success of the conditional overexpression of β-catenin specifically in the renal tubules of Tubcat mice.

Renal dysfunction in uninephrectomized Tubcat mice

To accelerate the renal injury in the animal model, six- to eight-week-old Tubcat mice and Cre$^{-/-}$ mice underwent uninephrectomy followed by tamoxifen injection (Figure 2A). Four weeks after transgenic induction, uninephrectomized (UNX) Tubcat mice expressed significantly more nuclear β-catenin in renal cortex (Figure 2B). UNX-Tubcat mice displayed significantly higher urine albumin-to-creatinine ratio (UACR; 130 ± 29 mg/ug vs. 45 ± 5.7 mg/ug) and blood urea nitrogen (BUN; 37.1 ± 3.2 mg/dL vs. 27.7 ± 1.9 mg/dL) compared to UNX-Cre$^{-/-}$ mice (Figure 2D), while there was no difference at baseline before uninephrectomy and tamoxifen injection (Figure 2C). Notably, we observed significant proteinuria and increase in serum BUN level in Tubcat mice, *de novo* to the transgenic effect (Supplementary Figure 2A&B). Acute kidney injury (AKI) markers including *Kim1*, *Cystatin C* and *Ngal* were all up-regulated in the kidney cortex of UNX-Tubcat mice vs. UNX-Cre$^{-/-}$ mice (Figure 2E). Periodic acid-Schiff (PAS) staining revealed glomerular

damage in UNX-Tubcat mice, as reflected by diffuse mesangial expansion (Figure 2F) with a higher glomerular damage score (Figure 2G). The glomerular histology associates with significant less nephrin expression, both in gene and protein manner (Figure 2H&I), in the UNX-Tubcat mice. UNX-Tubcat mice displayed significant higher urinary β2-microglobulin level (65.4 ± 11 ng/ml vs. 37.3 ± 1.7 ng/ml), a renal tubular damage marker, compared to uninephrectomized $Cre^{-/-}$ mice (Figure 2J). Collectively, these data demonstrated that enhanced β-catenin expression in renal tubules is detrimental and impairs renal function.

Overexpression of tubular β-catenin enhanced tubulointerstitial macrophage infiltration

Overexpression of tubular β-catenin in UNX-Tubcat mice resulted in 3-fold increase in macrophage infiltration (CD68+ cells) versus $Cre^{-/-}$ mice (Figure 3A). M1 macrophage markers (*Ly6c* and *Ccr2*) were significantly elevated in the kidneys of UNX-Tubcat mice compared to UNX-$Cre^{-/-}$ mice, while there was no difference in the M2 macrophage markers (*Cd163* and *Cd106*; Figure 3B). Enhanced tubulointerstitial macrophage infiltration in UNX-Tubcat mice was accompanied by up-regulated chemocytokine expression including CCL-2 and RANTES (Figure 3C). IHC staining of CCL-2 and β-catenin on serial kidney sections from UNX-Tubcat mice demonstrated the colocalization of CCL-2 and overexpressed β-catenin in renal tubules (Figure 3D). In line with this proinflammatory phenotype, the expression of TLR-4 and NLRP-3 was also increased in the renal cortex of UNX-Tubcat mice at both the gene and protein levels (Figure 3E&F).

Overexpressed β-catenin does not feedback or activate the non-canonical Wnt pathways

We investigated whether overexpression of β-catenin will impact other non-canonical WNT pathways. The non-canonical Wnt signaling related gene expression including *Camkii*, *Daam1*, *Plcb1*and *Ptk7* were investigated. We speculated *Camkii* and *Damm1* expression was significantly down-regulated in UNX-Tubcat kidney (Figure 4A). In Figure 4B, immunoblotting assays showed the phosphorylation level of several kinases involved in the non-canonical Wnt pathways, including c-Jun N-terminal kinase (JNK) and Ca^{2+}/calmodulin-dependent protein kinase II (CaMKII). We observed less phosphorylated CaMKII in the UNX-Tubcat kidney comparing to UNX-$Cre^{-/-}$ mice. In addition, we did not observe changes in phosphorylation of glycogen synthase kinase-3β (GSK-3β), an upstream regulator of β-catenin in UNX-Tubcat kidney (Figure 4C). Taking together, these data showed the overexpressed tubular β-catenin could not activate non-canonical Wnt pathways or induce feedback regulation of the canonical pathway.

Uninephrectomized Tubcat mice do not activate epithelial-mesenchymal-transition (EMT) or develop fibrosis in the kidney

To date, a number of articles has asserted the correlation between heightened tubular β-catenin expression and fibrogenesis during kidney injury. Treatment of β-catenin inhibitors could successfully ameliorate the EMT/fibrotic gene expression and extracellular matrix protein (ECM) deposition in kidney and thereby we studied the development of renal fibrosis via direct overexpression of tubular β-catenin in our mouse model. In Figure 5A, we examined the fibrotic markers including fibronectin, α-smooth muscle actin (α-SMA) and collagen I in experimental kidneys using immunoblotting assay. Surprisingly, no enhanced level of these fibrotic markers was detected in UNX-Tubcat mice comparing to UNX-$Cre^{-/-}$

mice. Moreover, there was no change in expression of two EMT markers, vimentin and E-cadherin, in the experimental kidneys (Figure 5B) which was in line with the fibrotic level.

Tubcat mice developed severe proteinuria during protein overload

To recapitulate the impact of protein overload in the renal tubules of CKD patients, an overload proteinuria model was established. After uninephrectomy and tamoxifen injection, high-dose of BSA (10mg/g body weight) or an equal volume of saline was injected intraperitoneally into UNX-Tubcat and UNX-Cre$^{-/-}$ mice for four weeks (Figure 6A). At baseline, all experimental mice had similar UACR and serum BUN level (Figure 6B). Four weeks after protein overload, BSA injected UNX-Cre$^{-/-}$ mice exhibited significantly higher UACR, serum BUN level compared to saline injected UNX-Cre$^{-/-}$ mice (Figure 6C). Importantly, BSA injected UNX-Tubcat mice displayed even higher UACR (1,500 ± 111 ug/mg vs. 689 ± 184 ug/mg), serum BUN levels (58.0 ± 3.7 mg/dL vs. 43.0 ± 5 mg/dL). Similar trend was also observed in urinary β2-microglobulin level (440 ± 74 ng/ml vs. 236 ± 40 ng/ml), suggesting more significant renal damage in UNX-Tubcat mice injected with BSA.

Enhanced tubular β-catenin triggers renal inflammation

Intrarenal expression of the *Catnb* allele (exon 3) was up-regulated in the BSA-injected Cre $^{-/-}$ mice compared to control group (Figure 6E), indicating that the enhanced transcriptional activity of the *Catnb* allele was due to BSA administration. As a result of Cre-lox recombination, its expression was significantly lower in Tubcat mice compared to Cre$^{-/-}$ mice when both were injected with BSA. Loss of exon 3 of *Catnb* allele stabilized β-catenin in the cell; thus conceivably more β-catenin could translocate into the nucleus and mediate its transcriptional function. Immunoblotting assay indicated the nuclear β-catenin level in the kidney was up-regulated in BSA-injected Cre$^{-/-}$ mice compared to the control, while BSA-injected Tubcat mice expressed the highest level of nuclear β-catenin (Figure 6F). Heightened β-catenin expression was mainly localized to the renal tubules of BSA-injected Cre$^{-/-}$ mice (Figure 6G). In Figure 6H, PAS staining revealed the renal architecture of experimental mice. We observed injured, dilated renal tubules and diffuse mesangial expansion in the kidney of BSA injected UNX-Cre$^{-/-}$ mice. Importantly, BSA injected UNX-Tubcat mice displayed further renal damage such as more dilated tubule with cast formation in the renal cortice.

IHC staining revealed increased tubulointerstitial infiltration by CD68+ macrophages after BSA injection in UNX-Cre$^{-/-}$ mice, and this was further enhanced in BSA injected UNX-Tubcat mice (Figure 7A). Real-time PCR confirmed that these infiltrating macrophages were of the M1 rather than the M2 phenotype (Figure 7B).

Up-regulated TLR-4/NLRP-3 and inflammatory chemocytokines in proteinuric Tubcat mice

Gene expression of *Tlr4*, *Ccl2*, *Il1b* and *Cxcl1* were all up-regulated in the renal cortex of BSA injected UNX-Tubcat mice compared to UNX-Cre$^{-/-}$ control animals (Figure 8A). Immunoblotting assay demonstrated that the protein levels of inflammatory chemocytokines (CCL-2, IL-17A and ICAM-1) were also significantly up-regulated in BSA injected UNX-Tubcat mice (Figure 8B), which was not observed in BSA injected UNX-Cre$^{-/-}$ mice.

Finally, renal cortical protein levels of TLR-4 and NLRP-3 were significantly increased in BSA injected UNX-Tubcat mice (Figure 8C). Collectively, these data demonstrated that activation of Wnt/β-catenin signaling in renal tubules promoted an inflammatory response during proteinuric nephropathy, possibly via the TLR-4/NLRP-3 inflammasome pathway.

DISCUSSION

CKD affects approximately 8–16% of the population worldwide. Proteinuria has long been known to be tubulotoxic and is an established biomarker that predicts progression and prognosis in various forms of diabetic and nondiabetic CKD. Wnt/β-catenin signaling, among a myriad of intracellular signal transduction pathways, has recently been studied in different renal cell types. Yet, reports on its ectopic activation in renal tubules and association with renal inflammation remain scarce.

We recently reported that Wnt/β-catenin signaling in renal tubules fluctuates during the different phases of experimental proteinuric nephropathy,[26] being evidently activated at the early phase. To characterize the role of tubular Wnt/β-catenin signals during overload proteinuria, we generated a mouse strain, the “Tubcat”, which could conditionally overexpress β-catenin specifically in the renal tubules. Not only are Tubcat mice tissue-specific, the temporal Cre/lox recombination circumvents any potential untoward consequences arising from overexpression in the early embryonic life. We characterized the Tubcat mice by several approaches, including PCR detection of *Cre* allele/*loxP* sites in genomic DNA and the mutant *Catnb* allele among different organs. This transgenic recombination deleted exon 3 from *Catnb* allele, thereby stabilized β-catenin exclusively in the renal tubules of Tubcat mice and enhanced β-catenin expression in the tubular nuclei.

In addition to its overarching importance in renal fibrosis, Wnt/β-catenin signaling also mediated renal inflammation. Here, Tubcat mice displayed aggravated renal dysfunction compared to $Cre^{-/-}$ mice and the renal injury could be accelerated by uninephrectomy surgery, as evident by the significant glomerular and tubular damage. Moreover, the expression of AKI markers (*Kim1, Cystatin C and Ngal*) was up-regulated in the renal cortex of uninephrectomized Tubcat mice, indicating that activated Wnt/β-catenin signaling in renal tubules is detrimental to the kidney. Our data lend support to studies on transgenic knock-out/overexpression of β-catenin in podocytes and renal tubules.[15, 20] These studies confirmed that ectopic activation of tubular Wnt/β-catenin signaling triggers different renal pathophysiological events during CKD progression.

It is substantial that overexpressed tubular β-catenin correlates with fibrogenesis in CKD animal models, and treatment of Wnt inhibitors has yielded a promising therapeutic effect on renal function. However, animal data regarding direct overexpression of tubular β-catenin on fibrogenesis is sparse. Additionally, the cross-talk between canonical and non-canonical Wnt pathways in kidney deserves further investigation. From our Tubcat mice, we did not speculate formation of fibrosis or enhanced EMT markers, or activation of non-canonical Wnt pathways. We hypothesized the overexpressed tubular β-catenin induces renal fibrosis partially via recruitment of resident macrophage into the kidney which potentially trans-differentiate to myofibroblast.[32] It has been documented elevated intracellular Ca^{2+} level is

followed by β-catenin translocation into nucleus in several cell lines.[33] Interestingly, we also observed suppressed CaMKII phosphorylation in UNX-Tubcat kidney which may indicate the activation of Wnt/β-catenin in renal tubules could interfere the Wnt/Ca^{2+} pathway.

Previous studies indicated that activated Wnt/β-catenin signaling could induce inflammatory cytokine production such as CCL-2 in breast cancer cells[34] and various organs.[35, 36] Particularly, β-catenin could interact with CCL-2 promoter and regulates its transcription level. Our study is the first to demonstrate the activation of the TLR-4/NLRP-3 inflammasome axis in the kidney by Wnt/β-catenin signaling in renal tubules. The expression of TLR-4, NLRP-3 and the downstream chemokines CCL-2[37] and RANTES[38] were all up-regulated in the kidney of UNX-Tubcat mice. Such inflammatory responses coincided with enhanced macrophage infiltration in the tubulointerstitium, a hallmark of renal inflammation. The pleiotropic function of polarized macrophages in the kidney has been well characterized in different nephropathies.[39] Ample evidence shows that M1 macrophages induce renal inflammation while M2 macrophages play a role in tissue repair. In UNX-Tubcat mice, we observed tubulointerstitial infiltration by M1 macrophages which is in line with the overexpression of various proinflammatory chemocytokines. We postulate the tubulointerstitial inflammation is influenced by overexpression of tubular β-catenin *per se*, then subsequently leading to proteinuria as an aftermath of tubular and glomerular damage.

Tubcat mice subjected to overload proteinuria recapitulate changes observed during CKD pathogenesis. We observed proteinuria and elevated BUN levels in non-transgenic mice challenged with protein overload. Notably, BSA injected UNX-Tubcat mice displayed further renal dysfunction and increased expression of tubular injury marker. In addition, tubular β-catenin expression was enhanced in the BSA injected UNX-$Cre^{-/-}$ mice but to a lesser extent compared to UNX-Tubcat mice. We suggest that the protein overload induces tubulointerstitial inflammation via induction of tubular β-catenin expression and such inflammatory response could further augment the glomerular and tubular injury. As a result, it perpetuates the vicious cycle of the heavy proteinuria formation during CKD progression.

In agreement with previous findings,[40] our BSA injected mice displayed renal inflammation as evident by M1 macrophage infiltration and activated TLR-4/NLPR-3 inflammasome axis in renal cortices. Numerous studies have demonstrated the inflammatory role of TLR-4 in CKD,[41] and the TLR-4 antagonist CRX-526 exerts reno-protective effects by ameliorating renal inflammation.[42] Here, we observed that TLR-4 gene expression correlated with the β-catenin level and enhanced expression of TLR-4/NLRP-3 in the renal cortex of Tubcat mice. BSA-injected Tubcat mice further overexpressed inflammatory chemocytokines (CCL-2, ICAM-1) which may conceivably accelerate renal inflammation. Furthermore, IL-17A[43] and *Cxcl1*[44] expression which is enhanced in the inflamed kidney of AKI models, was also up-regulated in the proteinuric Tubcat kidney. These findings support the notion that tubular Wnt/β-catenin signaling confers a pro-inflammatory state in the kidney during proteinuric nephropathy.

In summary, we demonstrated a proinflammatory role of Wnt/β-catenin signaling in renal tubules during overload proteinuria. Activated tubular Wnt/β-catenin signaling could induce

TLR-4/NLRP-3 related chemocytokines in the kidney and orchestrate the subsequent chemotaxis of macrophages into the tubulointerstitium.

METHODS

Animal model

The animal experiments were approved by the Committee on the Use of Live Animals in Teaching and Research (Laboratory Animal Unit, The University of Hong Kong) and followed stringently with the National Institute of Health Guide for the Care and Use of Laboratory Animals. Mice were housed in 12-hour light/12-hour dark cycle, ad libitum to food and water. Ksp-CreER^{T2} mice were generated by Dr. Peter Igarashi (The UT Southwestern O'Brien Kidney Research Core Center, Dallas, US).[45] The CreER^{T2} fusion protein was expressed exclusively under the kidney specific Ksp-cadherin (cadherin 16) gene promoter, thereby restricted in the renal tubules. The CreER^{T2} fusion protein consists of a Cre recombinase that carries an in-frame modified human estrogen receptor which could be activated by 4-hydroxytamoxifen.

The Catnb$^{lox(ex3)/lox(ex3)}$ mice were generated and characterized by Professor Makoto Mark Taketo (Kyoto University, Kyoto, Japan).[46] The Catnb$^{lox(ex3)/lox(ex3)}$ mice carry two loxP sites sandwiching the exon 3 sequence of *Catnb* alleles where the serine/threonine phosphorylation sites of β-catenin were transcribed. These phosphorylation sites regulate the degradation of β-catenin thus deletion of the exon 3 sequence could stabilize β-catenin in the desirable tissue cells.

Generation and characterization of Tubcat mice (Ksp-CreER^{T2}-Catnb$^{lox(ex3)/wt}$)

We generated the Tubcat mouse littermate which carried Ksp-CreER^{T2} and Catnb$^{lox(ex3)/wt}$ alleles by cross-breeding the Ksp-CreER^{T2} mice and Catnb$^{lox(ex3)/lox(ex3)}$ mice. Those mice without Ksp-CreER^{T2} allele served as negative control. All mice were administered 4-hydroxytamoxifen or tamoxifen dissolved in corn oil (Sigma-Aldrich, St Louis, MO, USA; 1mg/g body weight) for 5 consecutive days via intraperitoneal (i.p.) injection to induce the Cre-lox recombination. For protein overload model, Tamoxifen was given an hour before BSA injection during the first week to Tubcat and Cre$^{-/-}$ mice. Specifically, the activated Cre recombinase in the renal tubular cells excised the exon 3 sequence of *Catnb* allele (Catnb$^{\Delta(ex3)}$) leading to β-catenin stabilization in the renal tubules.

Genotyping of Ksp-CreER^{T2} transgenic mice and Catnb $^{lox(ex3)/lox(ex3)}$ mice

Genomic DNA was extracted from ear biopsies collected from mice and PCR based genotyping was performed with the HotStart Mouse Genotyping Kit (Kapa Biosystems, Woburn, MA, USA), followed by separation of the PCR products by agarose gel (Invitrogen, Carlsbad, CA, USA). *Cre* allele was confirmed by using the *forward primer 5′-AGGTTCGTGCACTCATGGA-3′* and *reverse primer 5′-TCGACCAGTTTAGTTACCC-3′* (235bp). Catnb *lox P* sites were verified by using *forward primer 5′-AGGGTACCTGAAGCTCAGCG-3′* and *reverse primer 5′-CAGTGGCTGACAGCAGCTTT-3′* (645bp: Catnb$^{lox(ex3)}$ and 412bp: Catnb^{wt}).

To verify the successful Cre-lox recombination after tamoxifen administration, genomic DNA extracted from various organs was analyzed by PCR with the *forward primer 5′-CATTGCGTGGACAATGGCTACTCA-3′ and reverse primer 5′-GGCAAGTTCCGGTCATCC-3′* (867bp: $Catnb^{wt}$ and ~500bp: $Catnb^{\Delta(ex3)}$). The *Catnb* mRNA expression (exon 3) was verified by quantitative real time PCR (qPCR). Protein expression of the normal β-catenin and the mutant β-catenin in kidney cortices was confirmed by immunoblotting assay.

Murine protein overload nephropathy model

The Tubcat mice and non-transgenic mice ($Cre^{-/-}$) were subjected to protein overload animal model as previously described.[26] Urine and blood serum were collected for the baseline before experiments. Male mice at 6–8 weeks of age were uninephrectomized under anesthesia and followed by intraperitoneal injection of low-endotoxin BSA (A-9430, Sigma-Aldrich) weekly for 5 consecutive days, up to 4 weeks. Equal volume of saline was injected to the disease control mice. After 4-week BSA injection, 24-hour urine and blood serum samples were collected for analysis. Tissues include kidney, spleen, heart and liver were harvested and snap frozen in liquid nitrogen and stored at −70°C. Half of the kidney was fixed with 10% formalin and embedded in paraffin for immunohistochemistry analysis.

Quantitative real-time PCR (qPCR) and immunoblotting assay

Cortical protein and total RNA were extracted from the frozen kidney tissues using NucleoSpin® Triprep (Macherey-Nagel, Duren, Germany). Nuclear and Cytosolic protein was fractionized by NE-PER® extraction kit (Thermo Scientific). The RNAs were reversely transcribed to cDNAs (High-Capacity cDNA Reverse Transcription Kit; Applied Biosystems, Carlsbad, CA, USA) followed by qPCR analysis. qPCR was performed using StepOnePlus™ Real-Time PCR Systems (Applied Biosystems) with SYBR Green reagent (Applied Biosystems) and specific primers (Table 1). Relative gene expression was calculated after normalization with β-actin expression. All experimental groups were compared to their respective control group using StepOne™ software v2.3 (Applied Biosystems). Equal amount of protein lysate was resolved in Bolt™ 4–12% gel and transferred to 0.2μm PVDF membrane. Membranes were blotted with 5% non-fat milk and followed by overnight incubation of primary antibody against β-catenin, E-cadherin (BD Transduction Laboratories™, San Jose, CA, USA), α-SMA, CCL-2, collagen I, RANTES, TLR-4, Vimentin (Santa Cruz Biotechnology, Santa Cruz, CA), NLRP-3, p-CamKII (Novus Biologicals, Littleton, CO), Histone H3, p-JNK, Total JNK, p-GSK-3β, total GSK-3β (Cell Signaling Technology, Beverly, CA, USA), nephrin (R&D Systems, Minneapolis, MN, USA), p-CamKII (Abcam, Cambridge, UK), fibronectin (Sigma-Aldrich), and β-actin (Thermo Scientific). After washing, the membranes were then incubated with matched horse radish peroxidase (HRP) conjugated secondary antibodies (Dako, Carpinteria, CA, USA) and visualized by ChemiDoc XRS+ system (Bio-Rad, Hercules, CA, USA) after incubation with Clarity™ Western ECL Substrate (Bio-Rad) for 5 minutes. Densitometries of protein bands were quantified by Image Lab™ software (Bio-Rad). Relative expression of target protein was normalized with β-actin or Histone H3 expression.

Immunohistochemistry staining

Paraffin-embedded kidney tissue was sectioned (4μm) and de-paraffinized then followed by rehydration with concentration gradient of ethanol. The sections were then proceeded to microwave-based antigen retrieval step in 10mM citrate buffer and quenched by 3% hydrogen peroxide for 10 mins. Primary antibody against β-catenin (BD Transduction Laboratories™), CCL-2 and CD68 (Santa Cruz Biotechnology) diluted in IHC diluent (Enzo Life Sciences, Farmingdale, NY, USA) was applied on the sections overnight and subsequently with the secondary peroxidase conjugated antibody (Dako). The sections were developed by DAB substrate (Dako) then counterstained with CAT hematoxylin (Biocare Medical, Walnut Creek, CA, USA), followed by dehydration with ethanol/xylene solution before mounting. Following co-immunohistochemical staining with β-catenin and Thiazide sensitive sodium chloride cotransporter (NCC; Millipore, Bedford, MA, USA the sections were developed by the MultiView® (mouse-HRP/rabbit-AP) IHC kit (Enzo Life Sciences) according to the kit manual. CD68+ cells were counted in at least 10 non-overlapping tubulointerstitial area (400 X; excluded glomeruli) and average for individual sample.

Histology

Paraffin-embedded kidney section was processed as mentioned followed by staining with periodic acid-Schiff solution (Sigma-Aldrich) to evaluate glomerular and renal tubular injury. At least 20 glomeruli from the kidney section were randomly selected and scored to evaluate glomerular damage. Glomerular damage index was graded as followings: 0, no sclerosis; 1, 10–25% mesangial expansion/sclerosis; 2, 25–50% mesangial expansion/sclerosis; 3, 50–75% mesangial expansion/sclerosis; 4, 75–100% mesangial expansion/sclerosis; The final score for each section was calculated as followings: Final scores = 0 × (% of grade 0 glomeruli) + 1 × (% of grade 1 glomeruli) + 2 × (% of grade 2 glomeruli) + 3 × (% of grade 3 glomeruli) + 4 × (% of grade 4 glomeruli).

Urine and serum biochemistry

Mouse urinary albumin was measured by Albuwell M (Exocell Inc., Philadelphia, PA, USA). Urinary or serum creatinine was measured by enzymatic assay: Creatinine LiquiColor Test (Stanbio Laboratory, Boerne, TX, USA). Serum blood urea nitrogen (BUN) was measured by QuantiChromTM Urea Assay Kit (BioAssay Systems, Hayward, USA). Urinary β2-microglobulin level was measured by ELISA kit (Lifespan Biosciences, Seattle, WA, USA).

Statistics

All data were expressed as mean ± SEM. One-way ANOVA with Tukey's multiple comparison test or two-sided t-test were employed to calculate the difference between experimental groups in GraphPad Prism v.6 (GraphPad Software, San Diego, CA). $p<0.05$ was considered statistically significant.

Supplementary Material

Refer to Web version on PubMed Central for supplementary material.

Acknowledgments

This study is supported by the National Natural Science Fund (NSFC) of China (grant no. 81570647), and by donations from Mrs. Rita T. Liu SBS of L & T Charitable Foundation Ltd & Indo Café, and Mr. Winston Leung. WHY is supported by an Endowment Fund established for the "Yu Professorship in Nephrology" awarded to SCWT, and a donation from Mr. KK Chan of Chi Lee Cement and Building Materials Co. Ltd, the Hong Kong Concrete Co. Ltd and the Continental Cement and Gypsum Co. Ltd. We thank Prof. Peter Igarashi, the University of Texas Southwestern O'Brien Kidney Research Core Center (NIHP30DK079328 and R37DK042921), IGBMC, and Dr. Pierre Chambon for providing the Ksp-CreER^{T2} mouse strain. We are also grateful to Prof. Makoto Mark Taketo from Kyoto University for providing the Catnb$^{lox(ex3)/lox(ex3)}$ mice. Part of the results from this study was presented in abstract form at the American Society of Nephrology Kidney Week, 2017, New Orleans, LA, US.

References

1. Heerspink HJ, Kropelin TF, Hoekman J, et al. Drug-Induced Reduction in Albuminuria Is Associated with Subsequent Renoprotection: A Meta-Analysis. J Am Soc Nephrol. 2015; 26:2055–2064. [PubMed: 25421558]
2. Baines RJ, Brunskill NJ. Tubular toxicity of proteinuria. Nat Rev Nephrol. 2011; 7:177–180. [PubMed: 21151210]
3. Li RX, Yiu WH, Tang SC. Role of bone morphogenetic protein-7 in renal fibrosis. Front Physiol. 2015; 6:114. [PubMed: 25954203]
4. Saito A, Sato H, Iino N, et al. Molecular mechanisms of receptor-mediated endocytosis in the renal proximal tubular epithelium. J Biomed Biotechnol. 2010; 2010:403272. [PubMed: 20011067]
5. Birn H, Christensen EI. Renal albumin absorption in physiology and pathology. Kidney Int. 2006; 69:440–449. [PubMed: 16514429]
6. Coombes JD, Mreich E, Liddle C, et al. Rapamycin worsens renal function and intratubular cast formation in protein overload nephropathy. Kidney Int. 2005; 68:2599–2607. [PubMed: 16316336]
7. Nagai J, Yamamoto A, Yumoto R, et al. Albumin overload induces expression of hypoxia-inducible factor 1alpha and its target genes in HK-2 human renal proximal tubular cell line. Biochem Biophys Res Commun. 2013; 434:670–675. [PubMed: 23587905]
8. Cao W, Zhou QG, Nie J, et al. Albumin overload activates intrarenal renin-angiotensin system through protein kinase C and NADPH oxidase-dependent pathway. J Hypertens. 2011; 29:1411–1421. [PubMed: 21558957]
9. van Timmeren MM, Bakker SJ, Vaidya VS, et al. Tubular kidney injury molecule-1 in protein-overload nephropathy. Am J Physiol Renal Physiol. 2006; 291:F456–464. [PubMed: 16467126]
10. Tang S, Leung JC, Abe K, et al. Albumin stimulates interleukin-8 expression in proximal tubular epithelial cells in vitro and in vivo. J Clin Invest. 2003; 111:515–527. [PubMed: 12588890]
11. Nikolic-Paterson DJ, Wang S, Lan HY. Macrophages promote renal fibrosis through direct and indirect mechanisms. Kidney International Supplements. 2014; 4:34–38. [PubMed: 26312148]
12. Clevers H, Nusse R. Wnt/beta-catenin signaling and disease. Cell. 2012; 149:1192–1205. [PubMed: 22682243]
13. Moon RT, Kohn AD, De Ferrari GV, et al. WNT and beta-catenin signalling: Diseases and therapies. Nature Reviews Genetics. 2004; 5:689–699.
14. Kestler HA, Kuhl M. From individual Wnt pathways towards a Wnt signalling network. Philos Trans R Soc Lond B Biol Sci. 2008; 363:1333–1347. [PubMed: 18192173]
15. Kato H, Gruenwald A, Suh JH, et al. Wnt/beta-catenin pathway in podocytes integrates cell adhesion, differentiation, and survival. J Biol Chem. 2011; 286:26003–26015. [PubMed: 21613219]
16. Lancaster MA, Louie CM, Silhavy JL, et al. Impaired Wnt-beta-catenin signaling disrupts adult renal homeostasis and leads to cystic kidney ciliopathy. Nat Med. 2009; 15:1046–1054. [PubMed: 19718039]
17. Rooney B, O'Donovan H, Gaffney A, et al. CTGF/CCN2 activates canonical Wnt signalling in mesangial cells through LRP6: implications for the pathogenesis of diabetic nephropathy. FEBS Lett. 2011; 585:531–538. [PubMed: 21237163]

18. Zhou L, Li Y, Zhou D, et al. Loss of Klotho contributes to kidney injury by derepression of Wnt/beta-catenin signaling. J Am Soc Nephrol. 2013; 24:771–785. [PubMed: 23559584]
19. Kawakami T, Ren SY, Duffield JS. Wnt signalling in kidney diseases: dual roles in renal injury and repair. Journal of Pathology. 2013; 229:221–231. [PubMed: 23097132]
20. Zhou D, Li Y, Lin L, et al. Tubule-specific ablation of endogenous beta-catenin aggravates acute kidney injury in mice. Kidney Int. 2012; 82:537–547. [PubMed: 22622501]
21. Zhou D, Tan RJ, Fu H, et al. Wnt/beta-catenin signaling in kidney injury and repair: a double-edged sword. Lab Invest. 2016; 96:156–167. [PubMed: 26692289]
22. De Langhe SP, Reynolds SD. Wnt signaling in lung organogenesis. Organogenesis. 2008; 4:100–108. [PubMed: 19279721]
23. Li VSW, Ng SS, Boersema PJ, et al. Wnt Signaling through Inhibition of beta-Catenin Degradation in an Intact Axin1 Complex. Cell. 2012; 149:1245–1256. [PubMed: 22682247]
24. Hao S, He W, Li Y, et al. Targeted inhibition of beta-catenin/CBP signaling ameliorates renal interstitial fibrosis. J Am Soc Nephrol. 2011; 22:1642–1653. [PubMed: 21816937]
25. He W, Dai C, Li Y, et al. Wnt/beta-catenin signaling promotes renal interstitial fibrosis. J Am Soc Nephrol. 2009; 20:765–776. [PubMed: 19297557]
26. Wong DW, Yiu WH, Wu HJ, et al. Downregulation of renal tubular Wnt/beta-catenin signaling by Dickkopf-3 induces tubular cell death in proteinuric nephropathy. Cell Death Dis. 2016; 7:e2155. [PubMed: 27010856]
27. Pereira CP, Bachli EB, Schoedon G. The Wnt pathway: A macrophage effector molecule that triggers inflammation. Current Atherosclerosis Reports. 2009; 11:236–242. [PubMed: 19361356]
28. Liu Y, Almeida M, Weinstein RS, et al. Skeletal inflammation and attenuation of Wnt signaling, Wnt ligand expression, and bone formation in atherosclerotic ApoE-null mice. American Journal of Physiology-Endocrinology and Metabolism. 2016; 310:E762–E773. [PubMed: 26956187]
29. George SJ. Wnt pathway: a new role in regulation of inflammation. Arterioscler Thromb Vasc Biol. 2008; 28:400–402. [PubMed: 18296599]
30. Wu HJ, Yiu WH, Li RX, et al. Mesenchymal Stem Cells Modulate Albumin-Induced Renal Tubular Inflammation and Fibrosis. PLoS ONE. 2014; 9:e90883. [PubMed: 24646687]
31. Liu FY, Li Y, Peng YM, et al. Norcantharidin ameliorates proteinuria, associated tubulointerstitial inflammation and fibrosis in protein overload nephropathy. Am J Nephrol. 2008; 28:465–477. [PubMed: 18176075]
32. Nikolic-Paterson DJ, Wang S, Lan HY. Macrophages promote renal fibrosis through direct and indirect mechanisms. Kidney Int Suppl (2011). 2014; 4:34–38. [PubMed: 26312148]
33. Thrasivoulou C, Millar M, Ahmed A. Activation of intracellular calcium by multiple Wnt ligands and translocation of beta-catenin into the nucleus: a convergent model of Wnt/Ca2+ and Wnt/beta-catenin pathways. J Biol Chem. 2013; 288:35651–35659. [PubMed: 24158438]
34. Mestdagt M, Polette M, Buttice G, et al. Transactivation of MCP-1/CCL2 by beta-catenin/TCF-4 in human breast cancer cells. Int J Cancer. 2006; 118:35–42. [PubMed: 16003740]
35. Silva-Garcia O, Valdez-Alarcon JJ, Baizabal-Aguirre VM. The Wnt/beta-catenin signaling pathway controls the inflammatory response in infections caused by pathogenic bacteria. Mediators Inflamm. 2014; 2014:310183. [PubMed: 25136145]
36. Reuter S, Beckert H, Taube C. Take the Wnt out of the inflammatory sails: modulatory effects of Wnt in airway diseases. Lab Invest. 2016; 96:177–185. [PubMed: 26595171]
37. Vilaysane A, Chun J, Seamone ME, et al. The NLRP3 inflammasome promotes renal inflammation and contributes to CKD. J Am Soc Nephrol. 2010; 21:1732–1744. [PubMed: 20688930]
38. Hu CY, Ding HY, Li YY, et al. NLRP3 deficiency protects from type 1 diabetes through the regulation of chemotaxis into the pancreatic islets. Proceedings of the National Academy of Sciences of the United States of America. 2015; 112:11318–11323. [PubMed: 26305961]
39. Tian S, Chen SY. Macrophage polarization in kidney diseases. Macrophage (Houst). 2015:2.
40. Wu HJ, Yiu WH, Li RX, et al. Mesenchymal stem cells modulate albumin-induced renal tubular inflammation and fibrosis. PLoS One. 2014; 9:e90883. [PubMed: 24646687]
41. Yiu WH, Lin M, Tang SC. Toll-like receptor activation: from renal inflammation to fibrosis. Kidney Int Suppl (2011). 2014; 4:20–25. [PubMed: 26312146]

42. Lin M, Yiu WH, Li RX, et al. The TLR4 antagonist CRX-526 protects against advanced diabetic nephropathy. Kidney Int. 2013; 83:887–900. [PubMed: 23423259]
43. Xue L, Xie K, Han X, et al. Detrimental functions of IL-17A in renal ischemia-reperfusion injury in mice. J Surg Res. 2011; 171:266–274. [PubMed: 20400117]
44. Chung AC, Lan HY. Chemokines in renal injury. J Am Soc Nephrol. 2011; 22:802–809. [PubMed: 21474561]
45. Patel V, Li L, Cobo-Stark P, et al. Acute kidney injury and aberrant planar cell polarity induce cyst formation in mice lacking renal cilia. Hum Mol Genet. 2008; 17:1578–1590. [PubMed: 18263895]
46. Harada N, Tamai Y, Ishikawa T, et al. Intestinal polyposis in mice with a dominant stable mutation of the beta-catenin gene. EMBO J. 1999; 18:5931–5942. [PubMed: 10545105]

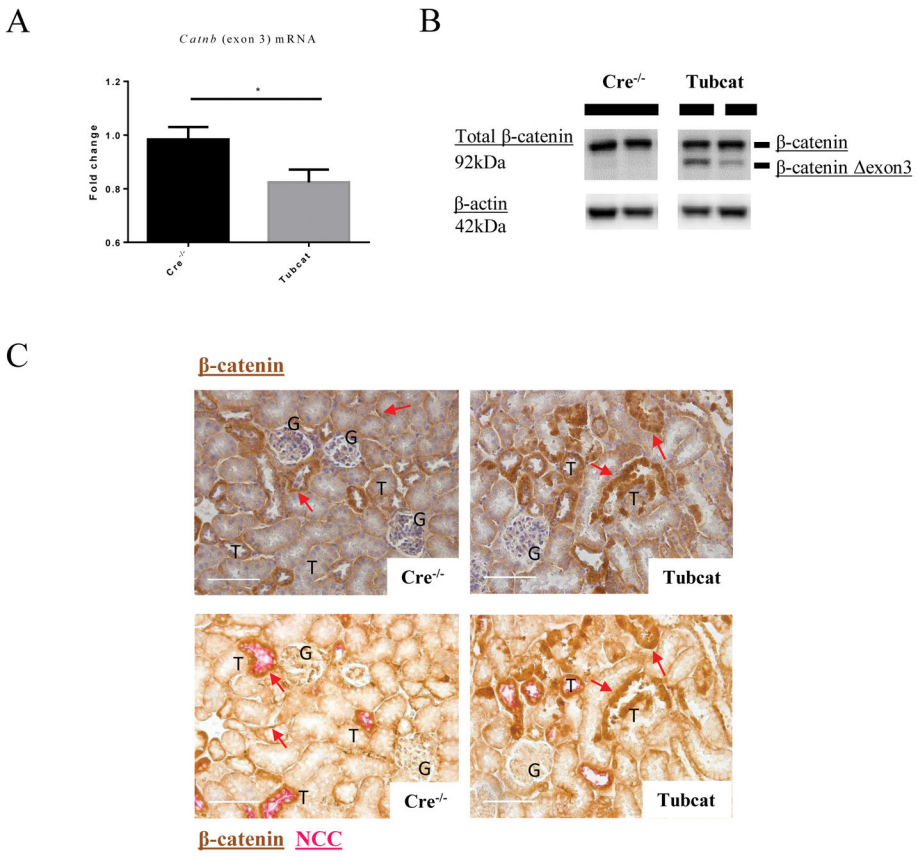

Figure 1. Tubcat mice overexpress β-catenin specifically in renal tubules after tamoxifen induction

(A) qPCR showed less mRNA expression of *Catnb* allele (exon 3) in the renal cortex of Tubcat mice after transgenic modification (n=5). (B) Expression of the native and mutant forms of β-catenin in renal cortical cells by immunoblotting. (C) Consecutive kidney sections revealed β-catenin overexpression in the renal tubules of Tubcat mice. Upper panels show the IHC staining of β-catenin (brown) and the lower panels show the co-staining of β-catenin (brown) and Na^+-Cl^- cotransporter (NCC, tubule marker; red). Red arrows indicate tubular β-catenin expression in $Cre^{-/-}$ and Tubcat mice, respectively. Bar scale = 250 μm. Results were expressed as means ± SEM. A two-sided t-test was used for comparison. G, glomerulus. T, renal tubules. M, DNA ladder. *p<0.05

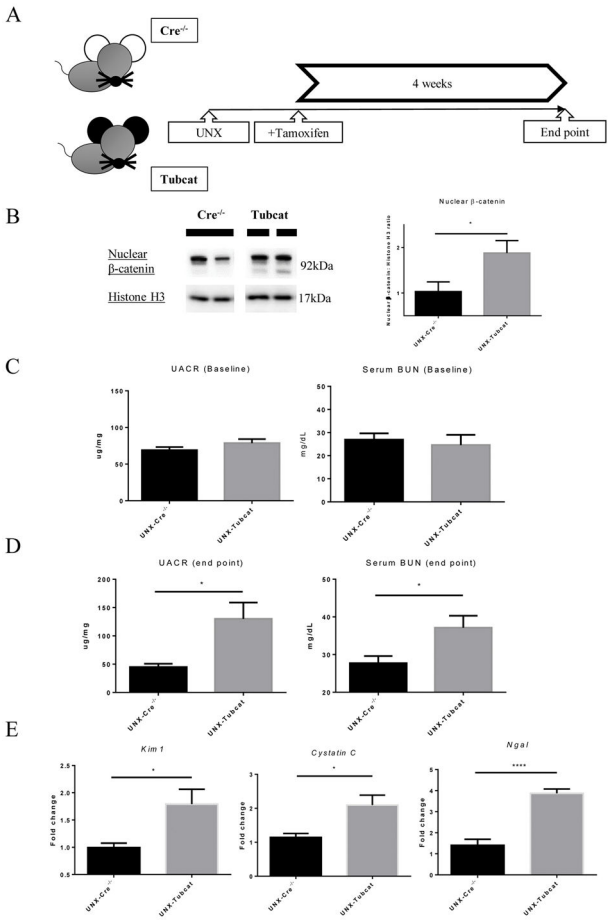

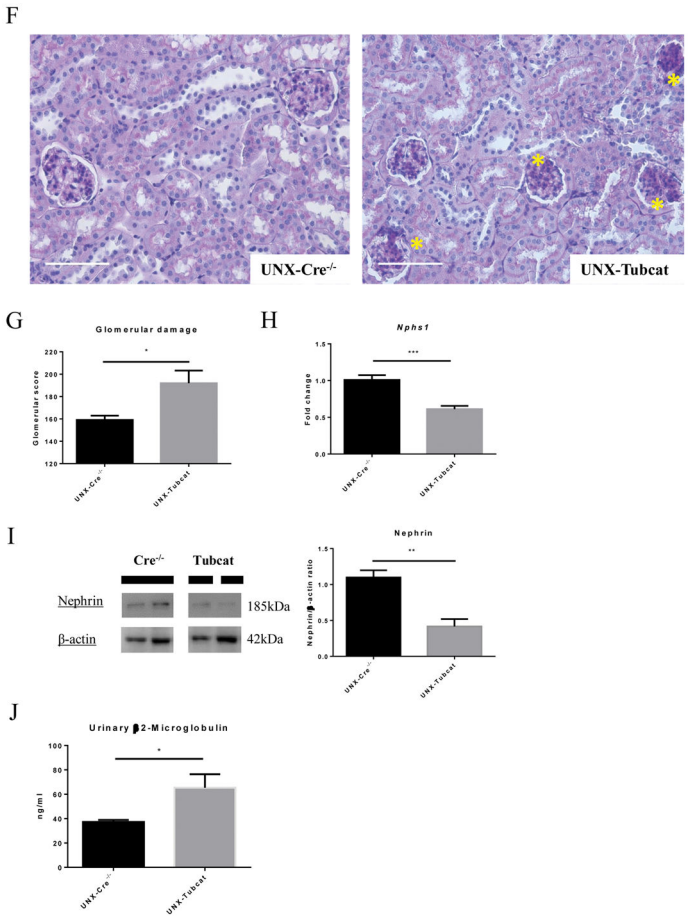

Figure 2. Renal dysfunction in uninephrectomized Tubcat mice 4 weeks after tamoxifen induction

(A) Schema of transgenic induction in Tubcat mice. (B) Expression of nuclear β-catenin in renal cortices of experimental mice (n=5). Representative immunoblots are shown. Urine albumin-to-creatinine ratio (UACR) and blood urea nitrogen (BUN) were measured at (C) baseline (n=5) and (D) 4 weeks after tamoxifen administration (n=5). (E) Renal cortical expression of AKI markers (n=5) in Tubcat and $Cre^{-/-}$ mice at experimental endpoint. (F) Representative periodic acid-Schiff (PAS) staining of kidney section from UNX-Tubcat and UNX-$Cre^{-/-}$ mice. Asterisks indicates the mesangial expansion. Bar scale = 250 μm. (G) Glomerular damage scoring of the kidney sections from the experimental mice (n=5). (H) Gene expression of *Nphs1* in renal cortices of uninephrectomized Tubcat and $Cre^{-/-}$ mice (n=5) 4 weeks after tamoxifen administration by qPCR. (I) Renal cortical protein expression of nephrin in the experimental mice (n=5) by immunoblotting assay. (J) Urinary β2-macroglobulin was measured in experimental mice 4 weeks after tamoxifen administration (n=5). Results were expressed as means ± SEM. A two-sided t-test was used for comparison. *p<0.05, **p< 0.01, ***p<0.0001

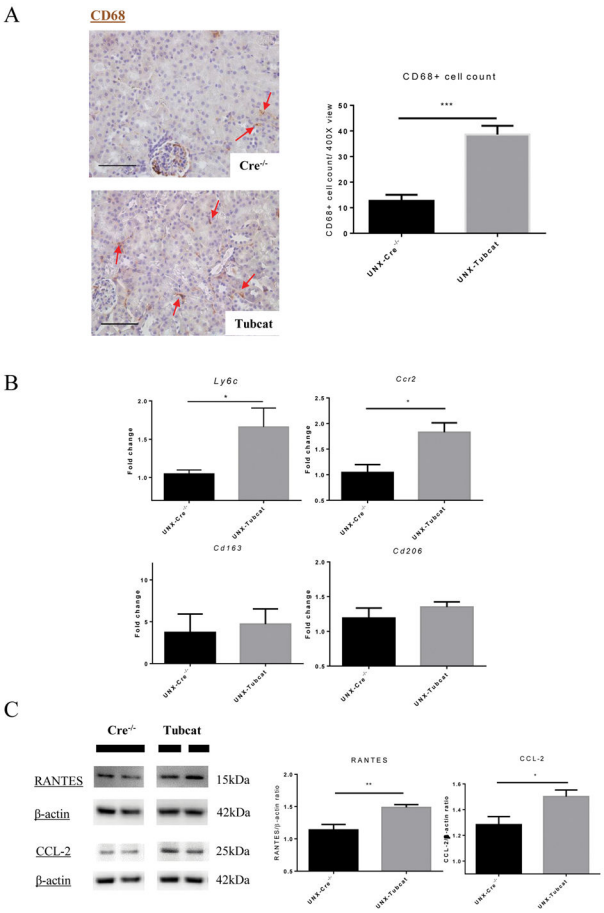

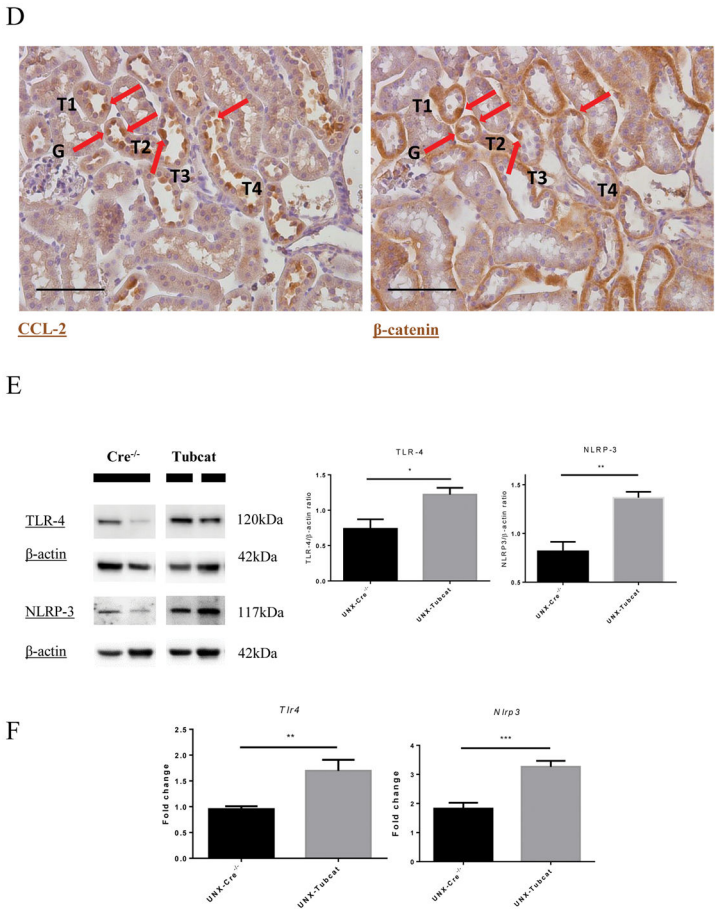

Figure 3. Renal inflammation in uninephrectomized Tubcat mice with enhanced cortical chemocytokine expression

(A) Immunohistochemical staining of CD68+ cells (red arrows) on kidney tissues. Average CD68+ cell counts on tubulointerstitial area (400X magnification) of Tubcat and $Cre^{-/-}$ mice (n=5). (B) Gene expression of M1 (*Ly6c* and *Ccr2*) and M2 (*Cd163* and *Cd206*) macrophage markers in renal cortices of Tubcat and $Cre^{-/-}$ mice (n=5) 4 weeks after tamoxifen administration by qPCR. Renal cortical expression of (C) RANTES, CCL-2, and (E) TLR-4 and NLRP-3 in experimental mice by immunoblottings (n=5). (D) Immunohistochemistry staining of CCL-2 and β-catenin on serial kidney sections from a Tubcat mouse by using different primary antibodies as annotated. Red arrows indicate the colocalization of CCL-2 and β-catenin detected in the same tubular cells. Bar scale = 250 μm. (F) Gene expression of TLR-4 and NLRP-3 by qPCR (n=5). Results were expressed as means ± SEM. A two-sided t-test was used for comparison. *p<0.05, **p< 0.01, ***p<0.0001

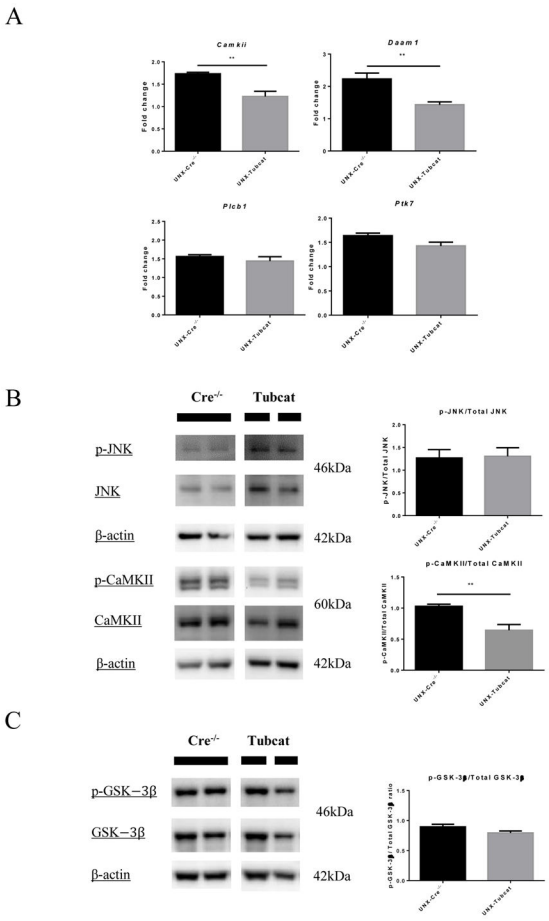

Figure 4. Expression of non-canonical Wnt pathway regulators in uninephrectomized Tubcat mice for 4 weeks

(A) Expression of non-canonical Wnt signaling related genes in renal cortices of uninephrectomized Tubcat and non-transgenic mice (n=5) by qPCR. Phosphorylation level of (B) JNK, CaMKII and (C) GSK-3β in renal cortices of uninephrectomized Tubcat and non-transgenic mice (n=5) by immunoblotting assay. Results were expressed as means ± SEM. A two-sided t-test was used for comparison. **p< 0.01

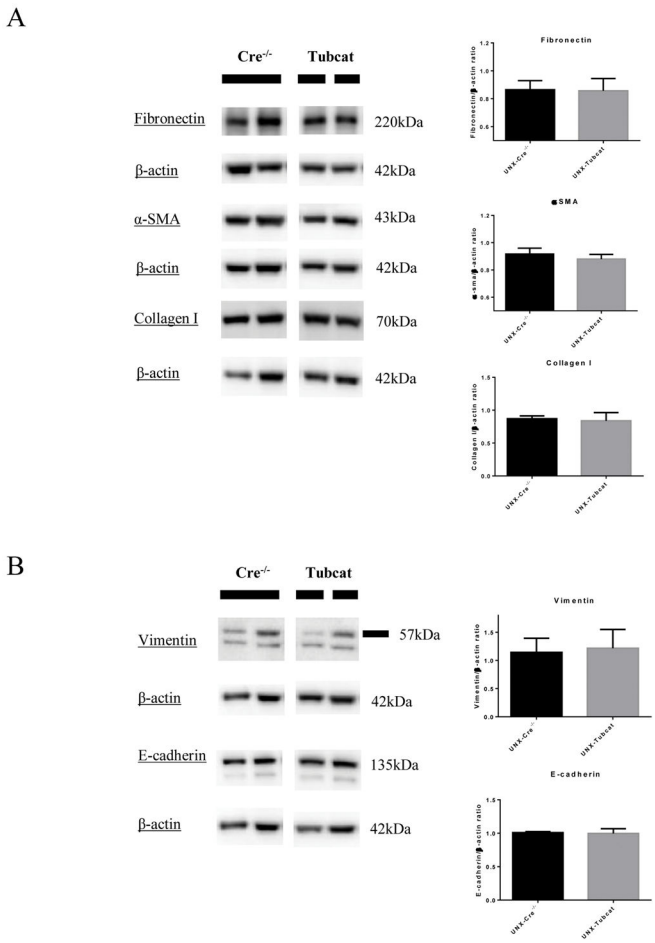

Figure 5. Fibrosis and EMT markers in UNX-Tubcat mice for 4 weeks

(A) Expression of fibrotic markers (fibronectin, α-SMA and collagen I) in renal cortices of UNX-Tubcat and UNX-Cre$^{-/-}$ mice (n=5) by immunoblotting assay. (B) Renal cortical expression of EMT markers (vimentin and E-cadherin) of uninephrectomized Tubcat and non-transgenic mice (n=5) by immunoblotting assay. Results were expressed as means ± SEM.

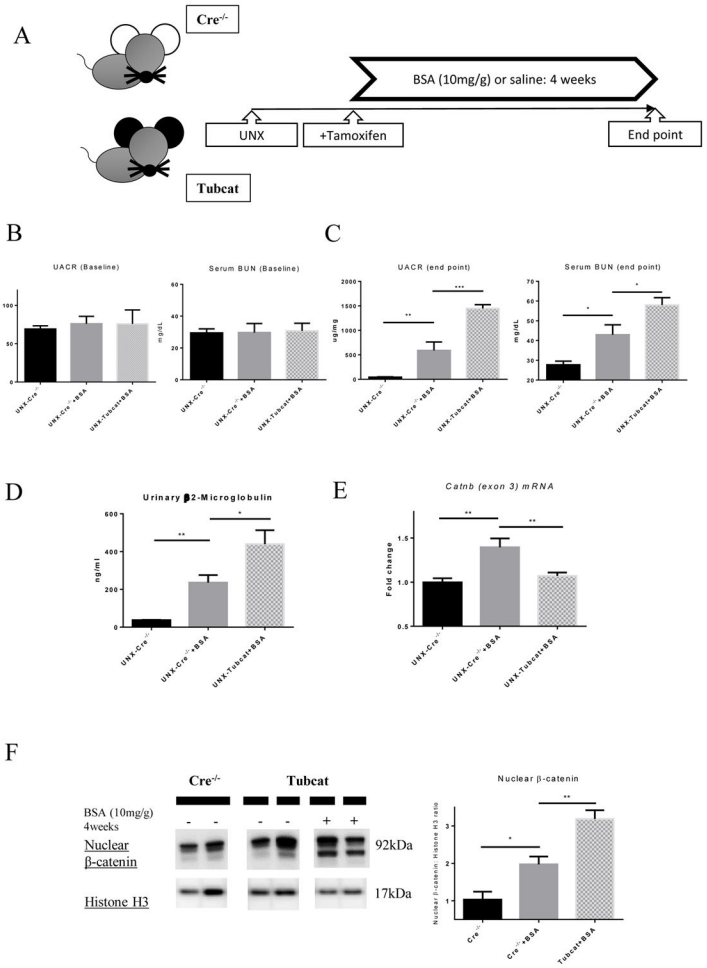

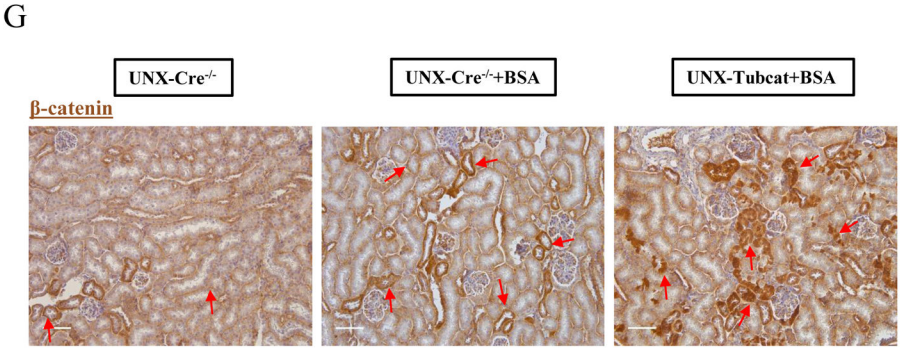

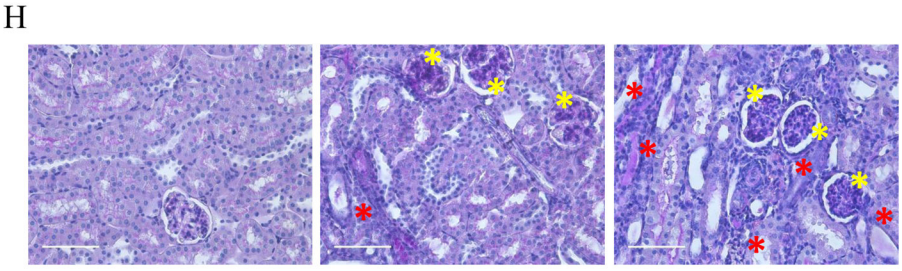

Figure 6. Induction of protein overload in uninephrectomized Tubcat and Cre$^{-/-}$ mice for 4 weeks

(A) Schema of UNX-Tubcat mice in protein overload model. UACR and BUN levels of experimental mice at (B) baseline (n=5) and (C) 4 weeks after BSA injection (n=5). (D) Urinary β2-macroglobulin measured in BSA injected UNX-Cre$^{-/-}$ mice and UNX-Tubcat mice at the experimental endpoint (n=5). (E) Renal cortical mRNA expression from *Catnb* allele (exon 3) by qPCR (n=5). (F) Both mutant and wild-type forms of nuclear β-catenin expression in the renal cortical lysate by immunoblotting (n=5). (G) Immunohistochemical staining of β-catenin on kidney tissues. Red arrows indicate β-catenin expression in tubules. Bar scale = 125 μm. (H) Representative periodic acid-Schiff (PAS) staining of kidney section from BSA injected UNX-Tubcat and UNX-Cre$^{-/-}$ mice. Yellow asterisks indicate the mesangial expansion and red asterisks indicate tubular injury. Bar scale = 250 μm. A One-way ANOVA was used for comparison. Results were expressed as means ± SEM. *p<0.05, **p< 0.01, ***p<0.0001

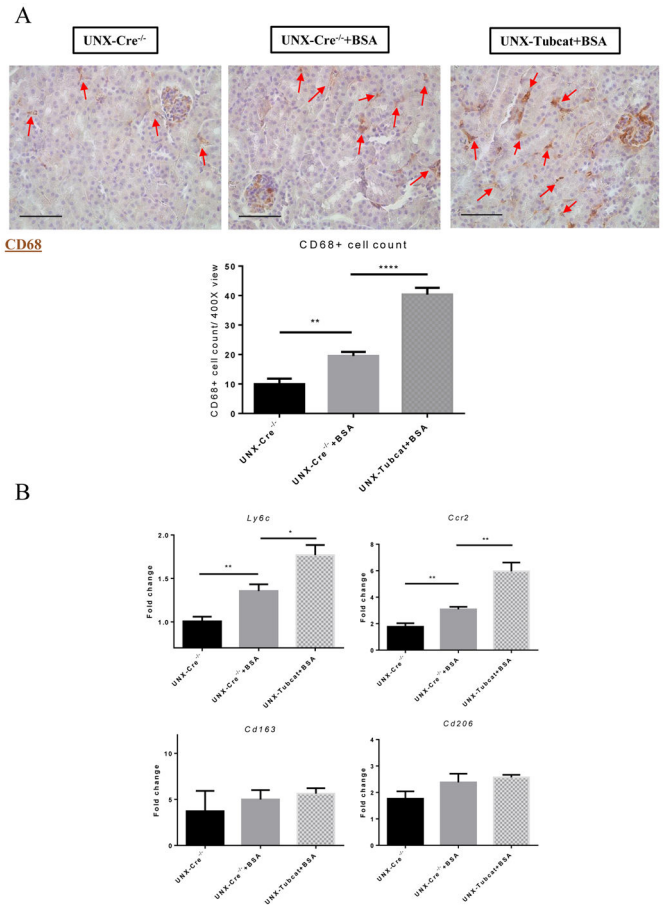

Figure 7. Increased tubulointerstitial macrophage infiltration in protein overloaded Tubcat mice

(A) CD68+ cells (red arrows) in kidney sections of protein overloaded animals and quantification (n=5). (B) Renal cortical expression of M1 and M2 macrophage markers in Tubcat and $Cre^{-/-}$ mice (n=5) by qPCR. Bar scale = 250 μm. Results were expressed as means ± SEM. A One-way ANOVA was used for comparison. *p<0.05, **p< 0.01, ****p<0.0001

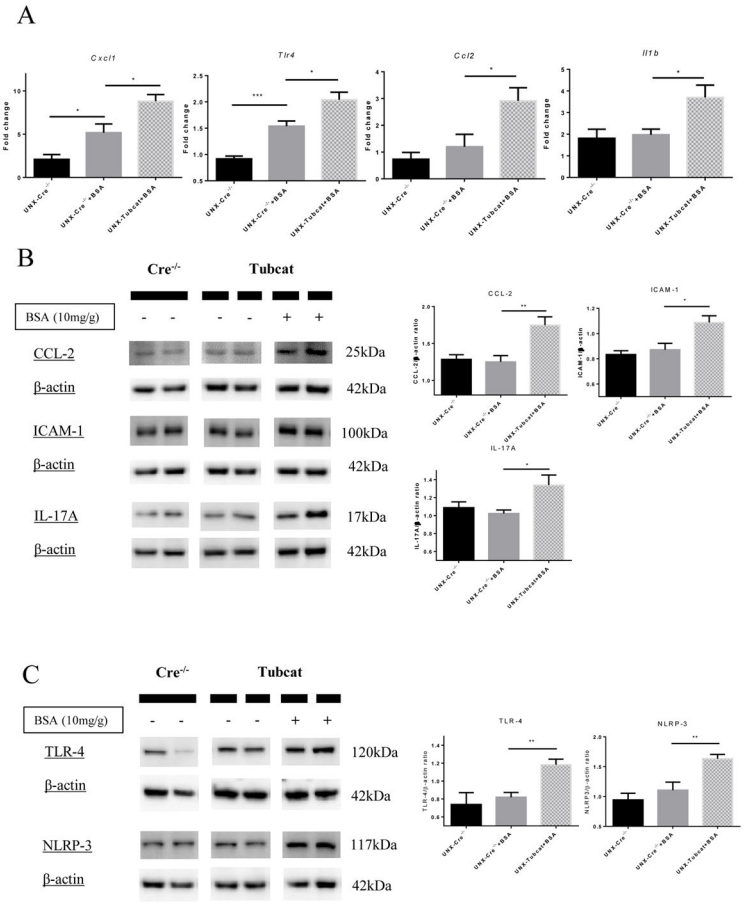

Figure 8. Induction of inflammatory chemocytokines and TLR-4/NLRP-3 in BSA-injected Tubcat mice

(A) Cortical gene expression of inflammatory chemocytokines (*Cxcl1*, *Tlr4*, *Ccl2* and *IL1b*) in BSA-injected mice by qPCR (n=5). Protein levels of (B) CCl-2, ICAM-1, IL-17A and (C) TLR-4 and NLRP-3 by immunoblotting of kidney cortical lysates (n=5). Results were expressed as mean ± SEM. A One-way ANOVA was used for comparison. *p<0.05, **p< 0.01, ***p<0.001

Table 1

Custom primers for quantitative real-time PCR

Gene	Primers
Actb	Forward: *5′-TCCATCATGAAGTGTGACGT-3′*
	Reverse: *5′-GAGCAATGATCTTGATCTTCAT-3′*
Catnb (exon 3)	Forward: *5′-GACGCTGCTCATCCCACTAA-3′*
	Reverse: *5′-CCACCTGGTCCTCATCGTTT-3′*
Camkii	Forward: *5′-ACCACTTCCTTCCACCACTT-3′*
	Reverse: *5′-TGAGATACAGCATTCCATACAAGA-3′*
Ccl2	Forward: *5′-CTCTTCCTCCACCACCAT-3′*
	Reverse: *5′-CTCTCCAGCCTACTCATTG-3′*
Ccr2	Forward: *5′-ATCCACGGCATACTATCAACATC-3′*
	Reverse: *5′-CAAGGCTCACCATCATCGTAG-3′*
Cd163	Forward: *5′-TGCTGTCACTAACGCTCCTG-3′*
	Reverse: *5′-TCATTCATGCTCCAGCCGTT-3′*
Cd206	Forward: *5′-AAGGCATGCGTTGCACATAC-3′*
	Reverse: *5′-ATTCTGCTCGATGTTGCCCA-3′*
Cystatin C	Forward: *5′-TGTTTGCACCAGGAGACAGT-3′*
	Reverse: *5′-AATTGAGCAAGGCATGGCAG-3′*
Cxcl1	Forward: *5′-TTGACGCTTCCCTTGGACAT-3′*
	Reverse: *5′-CTTTGAACGTCTCTGTCCCGA-3′*
Daam1	Forward: *5′-CACCTGCGAGTTGGTAACCT-3′*
	Reverse: *5′-GCTAATGAATGAGTGCGGCG-3′*
Il1b	Forward: *5′-TTCAGGCAGGCAGTATCA-3′*
	Reverse: *5′-CCAGCAGGTTATCATCATCA-3′*
Kim1	Forward: *5′-AAACCAGAGATTCCCACACG-3′*
	Reverse: *5′-GTCGTGGGTCTTCCTGTACTC-3′*
Ly6c	Forward: *5′-GCAGTGCTACGAGTGCTATGG-3′*
	Reverse: *5′-ACTGACGGGTCTTTAGTTTCCTT-3′*
Ngal	Forward: *5′-ACAACCAGTTCGCCATGGTA-3′*
	Reverse: *5′-AAGCGGGTGAAACGTTCCTT-3′*
Nlrp3	Forward: *5′-AGAGCCTACAGTTGGGTGAAATG-3′*
	Reverse: *5′-CCACGCCTACCAGGAAATCTC-3′*
Nphs1	Forward: *5′-CCCAACACTGGAAGAGGTGT-3′*
	Reverse: *5′-CTGGTCGTAGATTCCCCTTG-3′*
Plcb1	Forward: *5′-TCAAACCCAATCCGATATGTCAAT-3′*
	Reverse: *5′-AGCCTCCTTCTTTACTTCCTCTT-3′*
Ptk7	Forward: *5′-AATGCTGGAACCCTACACTTTG -3′*
	Reverse: *5′-CCCTGTGGCTCGTTGGAT-3′*
Tlr4	Forward: *5′-CATCCAGGAAGGCTTCCACA-3′*

Gene	Primers
	Reverse: *5′-GGCGATACAATTCCACCTGC-3′*